Measurements and calculations of ^{238}U$(n, xn\gamma)$ partial γ-ray cross sections

N. Fotiades, G. D. Johns, R. O. Nelson, M. B. Chadwick, M. Devlin, M. S. Wilburn, and P. G. Young
Los Alamos National Laboratory, Los Alamos, New Mexico 87545, USA

J. A. Becker, D. E. Archer, L. A. Bernstein, P. E. Garrett, C. A. McGrath,* D. P. McNabb, and W. Younes
Lawrence Livermore National Laboratory, Livermore, California 94550, USA

(Received 18 June 2003; published 6 February 2004)

Absolute partial cross sections for production of 45 discrete γ rays in the ^{238}U$(n, xn\gamma)$ reactions with $x \leqslant 4$ are reported for incident-neutron energies in the range 1 MeV$< E_n <$100 MeV. A germanium-detector array for γ-ray detection and the "white"-neutron source at LANSCE/WNR were used for the measurement. The energy of the incident neutrons was determined using the time-of-flight technique. The data are compared with previous measurements and with theoretical predictions up to E_n=30 MeV from the GNASH reaction model. The combination of experimental results with theoretical calculations provides a means to deduce the ^{238}U(n, n') reaction cross section.

DOI: 10.1103/PhysRevC.69.024601 PACS number(s): 25.40.Fq, 28.20.−v, 21.10.−k

I. INTRODUCTION

Measurement of the ^{238}U neutron inelastic scattering cross section is a challenge due to the many low-lying levels in ^{238}U and the competition with fission. Here we apply a technique that we developed to deduce the ^{239}Pu$(n, 2n)^{239}$Pu cross section from partial cross-section measurements to the case of inelastic scattering. This technique uses high-resolution γ-ray spectroscopy and detailed theoretical reaction modeling to infer reaction channel cross sections. In addition to providing information on nuclear reactions and structure, such data have many applications in technology.

Partial γ-ray cross sections for low-lying states (in particular, $2^+ \rightarrow H0^+$ ground-state transitions in even-even nuclei) often can be used to infer reaction channel cross sections accurately because a very large fraction (typically $\sim$90%) of all γ-ray decays pass through the 2^+ first-excited state. This technique has been used, for example, for ^{56}Fe$(n, xn\gamma)$ and other "medium-mass" nuclei [1]. For the more complicated cases of ^{207,8}Pb$(n, xn\gamma)$ reactions, GNASH nuclear reaction model calculations were tested and combined with the measured γ-ray data [2] to infer more accurate (n, xn) cross sections. ^{27}Al was also studied to test the GNASH code for lighter nuclei [3], and ^{16}O [4] and Be [5], where accurate model calculations are difficult, were measured as well.

In 1996 an initiative was taken to extend such studies to the much more difficult case of actinide nuclei [6]. For this effort Ge and BGO detectors of the former HERA spectrometer at LBNL [7] were transferred to LANL for a joint LANL/LLNL project. Eleven new planar-geometry Ge detectors were added to the new GEANIE (germanium array for neutron-induced excitations) spectrometer [6] and escape-suppression shields were used to reduce backgrounds. Because of their better resolution these planar detectors were essential for actinide studies.

The data reported here are part of the initial series of studies on ^{235}U [8], ^{238}U [9], and ^{239}Pu [10]. Preliminary results were previously reported [11]. Additional experiments on ^{196}Pt [12–14] and ^{92}Mo [15,16] have also been completed. All of the results obtained provide a database which is useful for many purposes including testing nuclear reaction model calculations in detail.

The relatively close spacing of the levels in ^{238}U and the background from fission neutrons makes direct measurements of neutron inelastic scattering difficult. However, accurate and extensive high-energy-resolution measurements of the emitted γ rays can provide useful information on the inelastic scattering cross section. Other (n, xn) $(x = 2, 3, 4, ...)$ reaction channels can be studied and those leading to even-mass uranium nuclei are particularly suitable for the prompt-γ-ray technique, because the level energies are typically large enough and the decays are intense enough that a large fraction of the decays are readily observable. Much more limited information is obtained for the odd-mass uranium products due to the high internal conversion rates for the many intense low-energy decays and the partitioning of the intensity among many different decay paths.

In the present work, GEANIE was used with the "white"-neutron source at the Los Alamos Neutron Science Center (LANSCE)/Weapons Neutron Research (WNR) facility [17] to detect γ rays from neutron-induced reactions over a wide range of incident-neutron energies (1 MeV$< E_n <$100 MeV). γ-ray energies were measured with high precision and absolute partial cross sections for production of these γ rays were accurately determined. From such data the cross sections for formation of specific exit channels in neutron-induced reactions can be deduced. The results are compared with theoretical reaction model calculations up to E_n=30 MeV and with previous experimental results for γ-ray cross sections from inelastic scattering of neutrons up to $E_n \sim 6$ MeV on ^{238}U reported in Refs. [18,19].

*Present address: Idaho National Engineering and Environmental Lab, Idaho Falls, Idaho 83415.

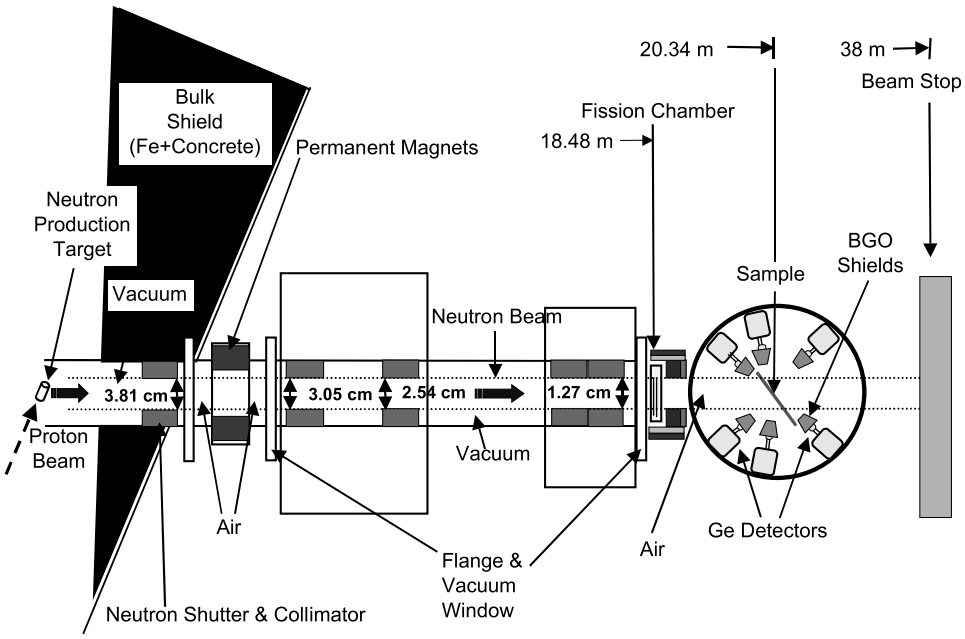

FIG. 1. Schematic diagram of the experimental setup used in both experiments described in the present work. The drawing is not to scale. Distances indicated by arrows are measured from the neutron production target.

II. EXPERIMENT

GEANIE is located 20.34 m from the WNR spallation neutron source on the 60R (60° right) flight path. A schematic diagram of the experimental setup is shown in Fig. 1. The neutrons are produced in a ^{nat}W spallation target driven by an 800-MeV proton beam with a time structure that consists of 625 to 725 μs-long "macropulses," with each macropulse containing subnanosecond-wide "micropulses," spaced every 1.789 μs. The energy of the neutrons was determined using the time-of-flight technique. GEANIE is comprised of 11 Compton suppressed planar Ge detectors [low-energy photon spectrometers (LEPS)], 9 Compton suppressed coaxial Ge detectors, and 6 unsuppressed coaxial Ge detectors. For the present measurements the detectors are arranged so that the LEPS are at angles nearly normal to the surface of the samples, in order to minimize attenuation of low-energy γ rays in the sample.

In a first run (in 1998) of the experiment, the target consisted of one ^{238}U foil, 730 mg/cm^2 thick. In a second run (in 1999), the target consisted of two ^{238}U foils, 840 mg/cm^2 thick in total, and four natural Fe foils, 165 mg/cm^2 thick in total, two in front and two at the back of the ^{238}U foils. In the 1999 run the samples were housed in a thick Monel ring with thin Be windows, the same as was used in a previously reported measurement with ^{239}Pu [12]. The Fe was included so that the cross section of the strong 846.8-keV line of ^{56}Fe from inelastic scattering could be used as a check on the absolute cross sections obtained (see discussion below). In both runs the target was rotated to 109° about the vertical with respect to the neutron beam. All ^{238}U foils used in the present work were 99.798% enriched in ^{238}U, the rest being mostly ^{235}U and very little ^{234}U.

The neutron flux on target was measured with a fission chamber, consisting of ^{235}U and ^{238}U foils [20,21], located 18.48 m from the center of the spallation target. The neutron fluences determined for each run versus neutron energy are shown in Fig. 2.

Absolute detector efficiencies were determined using a variety of calibrated γ-ray reference sources. Corrections for the finite beam spot size and γ-ray attenuation in the sample were modeled using the MCNP Monte Carlo radiation transport code [22]. The details of the modeling and source measurements are given in Ref. [23]. Data acquisition system "dead times" were measured using scalers and corrections were applied to the data. Typical dead time values were $\sim$45%. During the experiment the data were stored on magnetic tapes for subsequent offline analysis. A total of $\sim 7 \times 10^8$ γ singles and higher fold data were recorded (410×

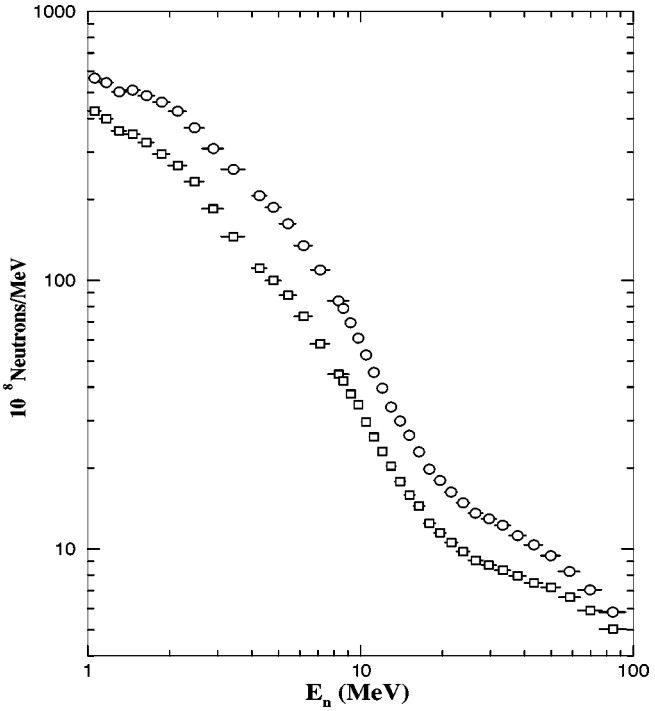

FIG. 2. Neutron fluences in the 1998 (squares) and 1999 (circles) runs deduced from the fission chamber data.

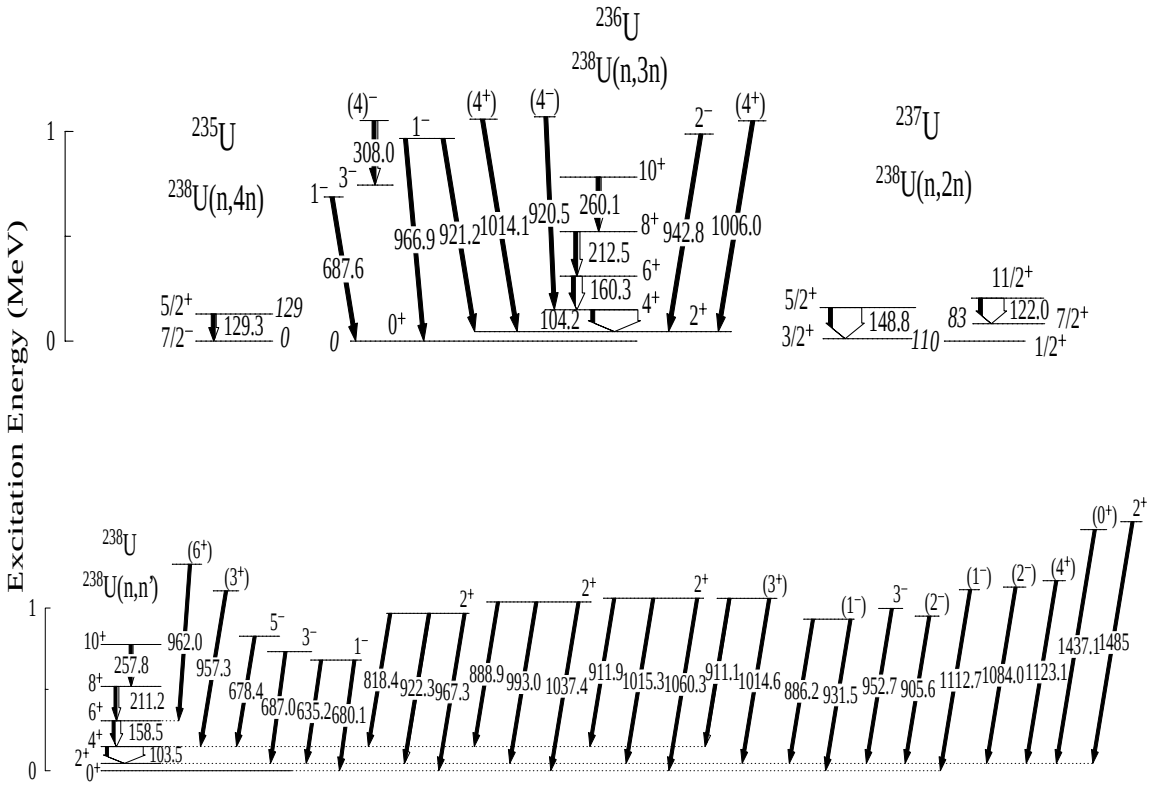

FIG. 3. Level schemes showing the transitions of $^{235-238}$U discussed in the present work. Level energies are given for the low-lying levels in the odd-mass isotopes. All γ-ray and level energies are given in keV. The white portion of the arrows indicates the fraction of the decay that is internally converted.

10^6 planar and 280×10^6 coaxial) in the second run of the experiment, while approximately one half this amount was collected in the first run.

III. ANALYSIS AND RESULTS

The production cross sections for a total of 45 γ rays of $^{235-238}$U isotopes were determined. All these transitions are included in the level schemes shown in Fig. 3. The cross sections as a function of incident neutron energy, deduced from the present work for the transitions in Fig. 3, are shown in Fig. 4. (For further details on the cross sections see Ref. [9].) Based on the shapes of the excitation functions in Figs. 4(xxii), 4(xxviii), and 4(xxxiii), it appears that we observe previously unknown γ rays in ^{236}U near E_γ=932 and 993 keV, and in ^{235}U at E_γ=1113 keV. The higher-energy peaks in Figs. 4(xxiv) and 4(xxv) are probably due to γ rays from fission fragments.

The off-line analysis consists of the following steps:

(i) Two-parameter arrays (matrices) of γ-ray energy E_γ versus time of flight (translated to neutron energy E_n) were built for the planar and coaxial detectors. By gating on the neutron-energy axis in these matrices γ-ray spectra in coincidence with certain neutron-energy bins were obtained. The fitting of the peaks in these spectra gives the yield (I_γ) of a γ ray at a certain neutron energy.

(ii) The neutron flux Φ versus neutron energy was deduced from the fission chamber. The uncertainty in the neutron flux is estimated at less than 4% for $E_n<14$ MeV and less than 8% for $E_n<30$ MeV.

(iii) The absolute partial γ-ray cross section was obtained using the relation

$$\sigma_\gamma(E_n) = \frac{I_\gamma \cdot \text{Dead } T_\gamma \cdot (1+\alpha_\gamma) \cdot C_\gamma}{\Phi(E_n) \cdot \text{Dead } T_\Phi \cdot \epsilon_\gamma \cdot t}, \tag{1}$$

where σ_γ is in mb, I_γ is the yield of a γ ray in counts/MeV, Φ is the incident neutron fluence in neutrons/MeV, ϵ_γ is the detection efficiency of the array for the particular γ-ray energy corrected for attenuation within the target and holder [23], α_γ is the conversion coefficient for the particular γ ray, C_γ is the angular-distribution correction (see Ref. [9]), and t is the target thickness in atoms/mb.

Dead T_γ and Dead T_Φ are the dead time corrections for the detection of γ rays from the array and neutrons in the fission chamber, respectively, determined by monitoring the count-rate of each individual detector in the array using scalers gated by the beam macropulse. The dead time includes both electronic dead time during ADC conversion and readout and pileup losses. The ADC conversion and readout constituted the majority of the dead time. The measured dead time for γ rays in the Ge detectors was greater than that for

TABLE I. Estimated cross-section systematic uncertainties in the present work.

	1998 Data (%)	1999 Data (%)
E_γ (keV)	$\delta\epsilon_\gamma$[a]	$\delta\epsilon_\gamma$[a]
100–400 (Planars)	5	5
600–750 (Coaxials)	10	11
751–900 (Coaxials)	9	10
901–1200 (Coaxials)	8	9
>1200 (Coaxials)	7	8
E_n (MeV)	$\delta\Phi(E_n)$	$\delta\Phi(E_n)$
1–4	1.0	0.8
4–8	1.5	1.0
9–19	2.0	1.4
20–50	1.5	1.2
51–100	1.2	1.1
δt	0.3	0.3
δ Dead T_γ	0.1	0.1
δ Dead T_Φ	0.2	0.15
Additional fluence uncertainty[b]	5	5

[a]Includes uncertainties in the γ-ray absorption in the sample, finite beam size effects, as well as detector efficiency uncertainties.
[b]Includes uncertainties in the fission foil thickness, fission cross section, and ionization chamber efficiency.

neutrons in the fission chamber. The cross section depends only on the ratio of the dead time corrections and this correction increased the cross-section values by ~15%. Distortion of the time-of-flight spectra due to the one stop per start TDC operation is calculated to be small.

The uncertainties in the cross section values reported in this work are statistical from the yield of a γ ray, I_γ, in Eq. (1). The systematic uncertainties for the rest of the variables in Eq. (1) are summarized in Table I. Wrap-around (time-frame overlap of lower-energy neutrons from a previous beam pulse) occurs in the present experiment at ~650 keV incident-neutron energy. Therefore, due to the threshold for fission and other neutron-induced reactions on ^{238}U, wrap-around could be a problem only in the inelastic channel and only for cross sections of transitions originating from levels with excitation energy below 650-keV (first four excited states of ^{238}U in Fig. 3). However, given the high spin of these states (the transition deexciting the 2^+ state has not been studied in the present work), the contribution of the wrap-around problem for these transitions is expected to be insignificant. Moreover, no corrections have been made to account for secondary effects (such as multiple scattering and emission of fission neutrons) in the target. Such effects were modeled using MCNP and a technique described previously [4], and account for less than 4% of the observed cross sections at 20 MeV incident neutron energy. (In the present case the effects of fission neutrons higher in energy than the incident neutron were neglected.) For $E_n > 100$ MeV the statistics were generally inadequate for γ-ray yields I_γ to be obtained through reliable fitting. An exception is the 158.5 -keV transition for which the cross section was deduced up to $E_n = 200$ MeV (see Ref. [9]).

TABLE II. Fission-barrier parameters used in the calculations.

Nucleus	Height[a]	Height[b]	Curvature[a]	Curvature[b]
^{239}U	6.25	6.00	0.75	0.50
^{238}U	5.83	5.33	0.50	0.50
^{237}U	6.03	5.63	0.50	0.50
^{236}U	6.10	5.90	0.50	0.50
^{235}U	6.00	5.90	0.85	0.55

[a]The inner barrier. Values are given in units of MeV.
[b]The outer barrier. Values are given in units of MeV.

IV. CALCULATIONS

The GNASH reaction model code, used here to predict cross sections for the transitions studied in the present work, includes preequilibrium, direct and fission nuclear reaction models coupled with a statistical Hauser-Feshbach calculation [24]. GNASH also includes multiple preequilibrium particle emission as well as angular momentum conservation for all emitted particles. GNASH predicts reaction and level cross sections, isomer ratios and spectra for γ rays, neutrons, and charged particles. Currently, the fission model for actinide nuclei and hence the cross-section calculations are limited to energies below 30 MeV incident neutron energy. However, work is planned to extend this limit to ~150 MeV. In the present GNASH calculations, results from direct ^{238}U (n, total) [25], $(n, 2n)$ [26], and $(n, 3n)$ [27] measurements were used to constrain the input parameters of the calculations to reproduce the total reaction cross section, and to a lesser extent to reproduce the $(n, 2n)$ and $(n, 3n)$ channel cross sections.

In the GNASH calculations of neutron reactions on ^{238}U, it is important to use an accurate coupled-channel (deformed) optical potential, because this determines the reaction cross section, the direct scattering cross sections to the coupled rotational states, and is also used to generate transmission coefficients for the Hauser-Feshbach calculations. Our optical model parameters given in Ref. [28] were obtained by fitting neutron total, elastic, and reaction cross-section measured data, using three coupled states. The fission model in GNASH uses double-humped inverted parabolas for the barriers, and the transition states at fission are entered as input, above which a statistical level density prescription is used. These transition states are obtained from nuclear structure predictions of the quasiparticle and collective excitations at the saddle points. Collective enhancements to the level densities due to breaking of nuclear shape symmetries are included, with a damping out of this effect at high excitation energies (above 15 MeV) as suggested by the microscopic calculations of Jensen [29]. The fission barrier heights and curvatures can be obtained from compilations based on neutron fission measurements and values inferred from direct transfer reactions. We also performed a systematic study of neutron reactions, including fission, for the chain of uranium isotopes from ^{232}U up to ^{238}U [30]—for instance, neutron

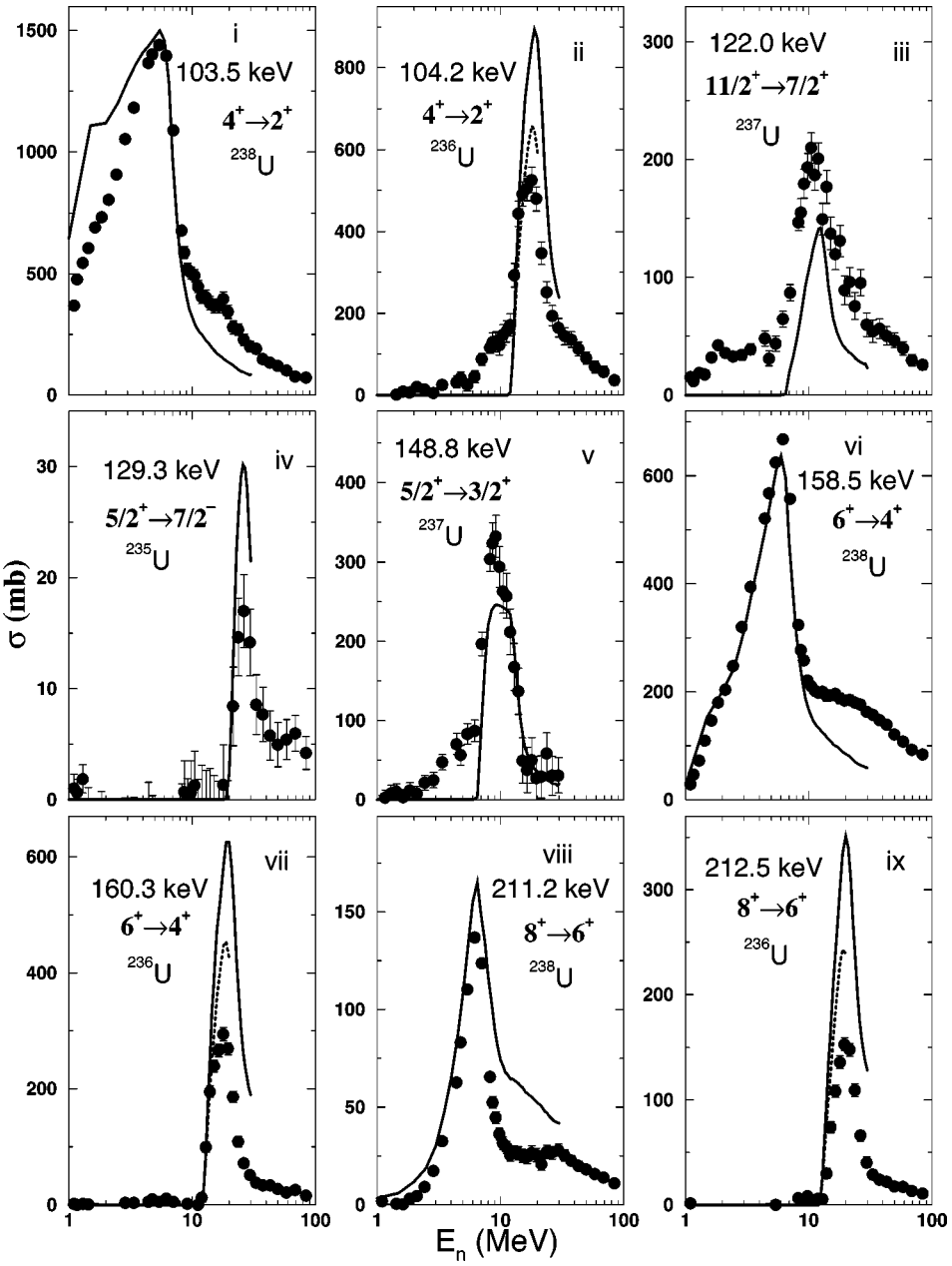

FIG. 4. Absolute partial cross-section values as a function of incident neutron energy for all transitions in Fig. 3, except 308.0- and 1006.0-keV transitions of ^{236}U which are weak (maximum cross section less than 20 mb [9]). Solid lines represent GNASH predictions [24]. For the transitions in the ground-state band of ^{236}U, the dotted lines represent the GNASH predictions normalized to the evaluated total $(n, 3n)$-channel cross section (see Fig. 5). In the cases where the transitions are doublets from the same isotope, the individual predictions are also presented in dotted and dashed lines. These transitions are as follows: in (xx), 911.1 keV (dotted) and 911.9 keV (dashed) transitions; in (xxi), 920.5 keV (dashed) and 921.2 keV (dotted) transitions; and in (xxix), 1014.6 keV (dotted) and 1015.3 keV (dashed) transitions. The arrows in (xxii), (xxviii), and (xxxiii) indicate previously unknown γ rays (see text). Finally, in (xxi), the size of the experimental points for higher neutron energies has been intentionally reduced so that the dotted line can be clearly seen in the figure.

reaction data on ^{235}U provides valuable information on barrier heights for ^{235,236}U, which are needed in the present work for modeling fission following the emission of three and four prefission neutrons. The parameters of the barriers we use are given in Table II.

There exist a number of measurements of $(n, 2n)$ and $(n, 3n)$ reaction channels for neutrons on ^{238}U. Since this paper provides a study of the γ-ray deexcitation cross sections in these channels, it is important to understand how the GNASH model calculations predict the overall channel cross section—if, for instance, our calculations overpredict the $(n, 3n)$ reaction channel cross section, then one would expect the calculations to also overpredict the $(n, 3n\gamma)$ cross sections. We show our calculations of the $(n, 2n)$ and the $(n, 3n)$ cross sections in Figs. 5 and 6, respectively, together with experimental data for these reaction channel cross sections. While Fig. 5 shows a reasonably good description of the $(n, 2n)$ cross section, in Fig. 6 the calculations do appear to

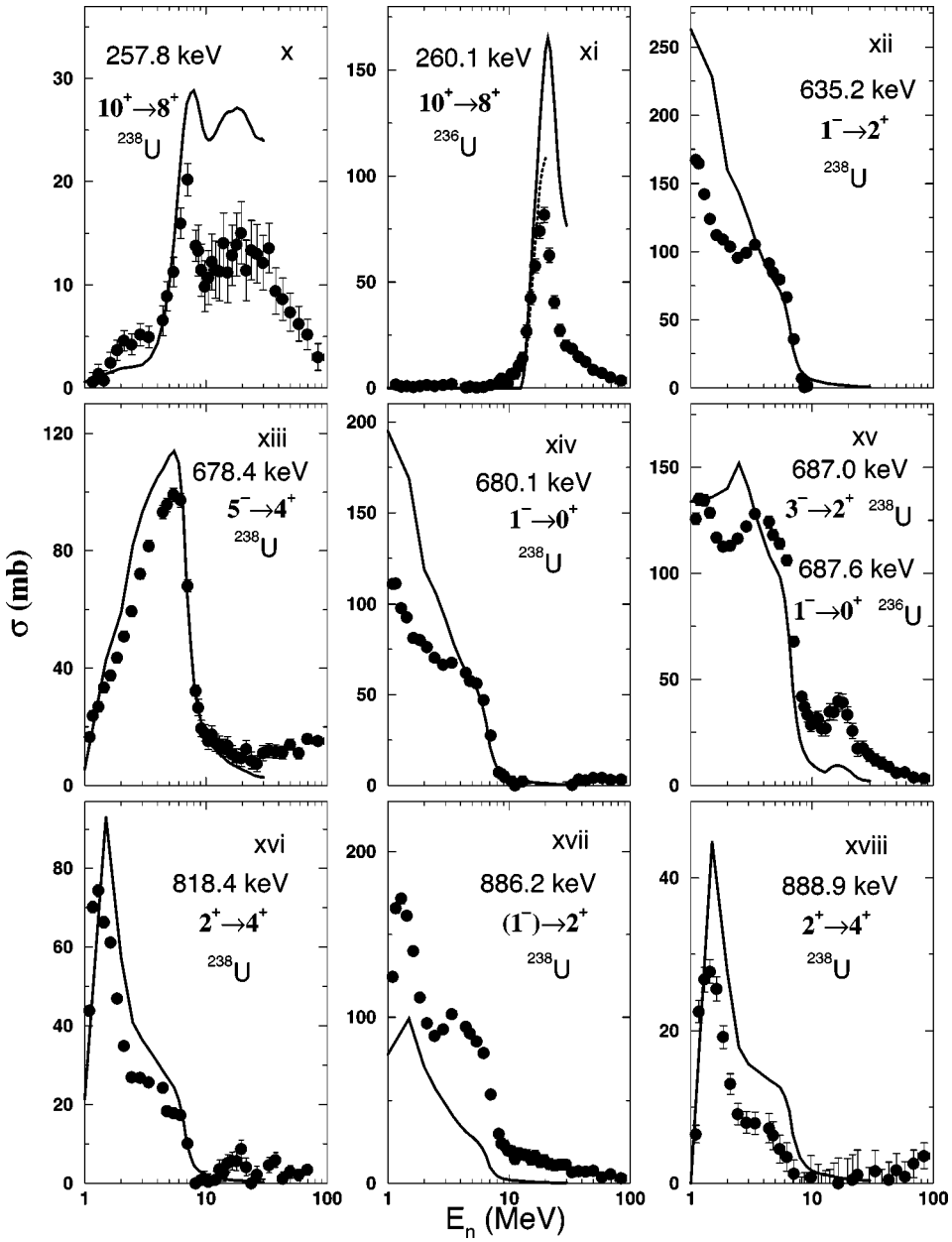

FIG. 4. (*Continued*).

overpredict the $(n, 3n)$ cross section (though the experimental database is small), and thus may be expected to exceed the partial γ-ray cross sections also. Due to the additional factors of spins, parities, branching ratios, and structure effects, correct calculation of individual partial γ-ray cross sections is more difficult.

V. DISCUSSION

In this section we compare the present data with other γ-ray cross-section measurements. We find generally good agreement with previous data with a few notable differences. Next we compare our data with the GNASH calculations of the γ-ray partial cross sections. Fairly good agreement is observed for the inelastic partial cross sections, although a deviation with increasing angular momentum is observed for the ground-state rotational band with the calculations exceeding the measurements significantly for the $10^+ \rightarrow 8^+$ transition. For the $(n, 3n)$ channel, as expected from the direct $(n, 3n)$ measurements, the calculations exceed the measurements significantly. Especially for the states of angular momenta greater than 4, the calculated cross sections are almost a factor of 2 greater than the data, but this is only a very small fraction of the channel cross section and for other states there is often a reasonably good agreement. Due to the observation of only a few γ rays from the odd-mass products ^{235}U and ^{237}U representing a very small fraction of the $(n, 4n)$ and $(n, 2n)$ channel cross sections, we cannot conclude much from the comparisons. Using the summed paral-

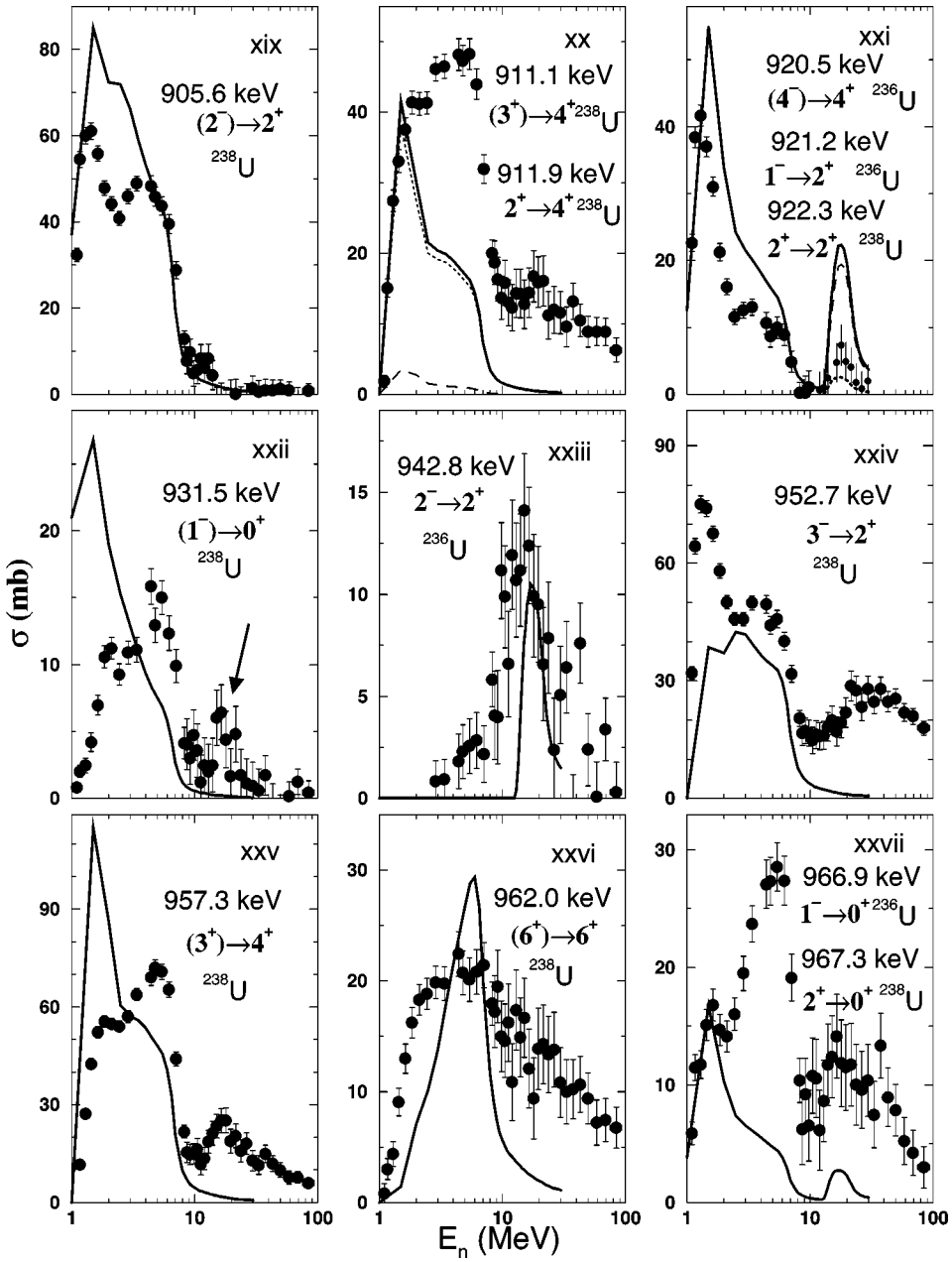

FIG. 4. (*Continued*).

lel γ-ray partial cross sections and the calculated ratio of the sum to the total, we deduce the ^{238}U(n, n')^{238}U channel cross section. This technique is similar to that used previously to determine the ^{239}Pu($n, 2n$)^{238}Pu channel cross section [10]. Lastly, we discuss the observed weak population of the $K^{\pi}=4^{-}$ state in ^{236}U in contrast to the much stronger population of a similar state in the ^{238}Pu isotone.

A. Comparison with other data

In Fig. 7 the results of the present work are compared with partial γ-ray cross sections obtained in inelastic scattering of neutrons [18,19] up to $E_n \sim 6$ MeV on ^{238}U. The results of Olsen *et al.* [18] are on average somewhat lower in magnitude than the present results for $E_n > 2$ MeV. Surprisingly, for three of the stronger lines the agreement with Olsen *et al.* is poor [see Figs. 7(i), 7(xiii), and 7(xv)]. In the case of $E_\gamma = 1015$ keV, two γ rays contribute to the observed yield. Larger differences (in magnitude but not in excitation function shape) were observed between the present results and the γ-ray cross sections obtained by Voss *et al.* [19], with their cross sections being much smaller in magnitude.

The preliminary results from the present data reported in Ref. [11] differ slightly from the results reported here due mainly to the following three changes in the analysis implemented after the publication in Ref. [11]: (i) the background subtraction in the fission chamber data was changed to correct an oversubtraction for $E_n < 4$ MeV resulting in lower

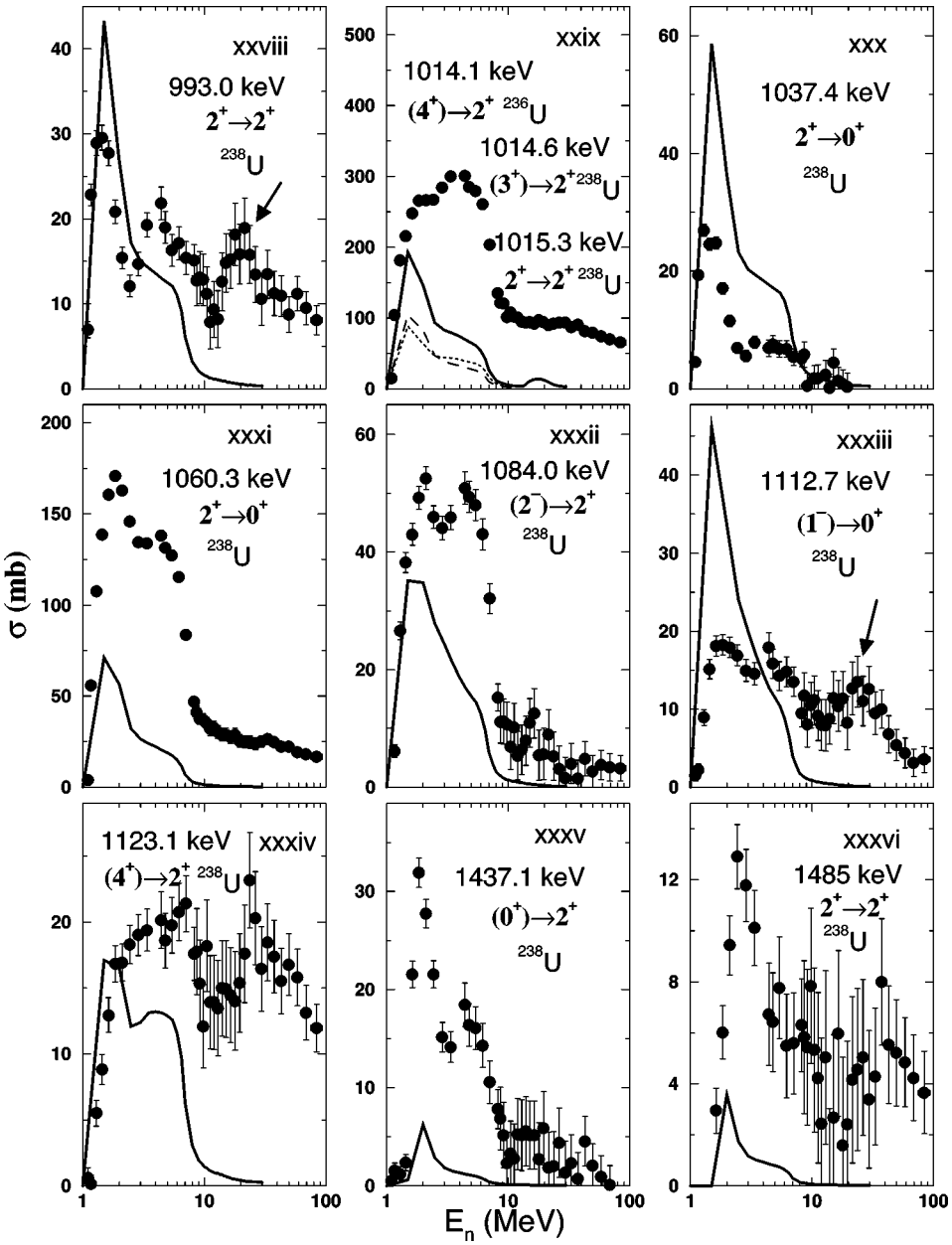

FIG. 4. (*Continued*).

cross-section values in the present data, (ii) weighted averages between the 1998 and 1999 datasets were implemented in the results presented here, as opposed to simple averages used in Ref. [11], and (iii) corrections were made for γ-ray attenuation in the Monel housing used in the 1999 dataset.

In order to check for systematic uncertainties in our method of measuring γ-ray cross sections, the results for the cross section of two transitions (846.8 and 1810.7 keV) of ^{56}Fe were compared to the evaluated cross section for these transitions at $E_n = 14.5$ MeV [31] (see Fig. 8). The evaluated cross sections at $E_n = 14.5$ MeV, for production in natural Fe, are in good agreement with the observed values in the present experiment. As a check on our cross sections as a function of incident neutron energy, in Fig. 8 we compare our excitation function for the 846.8 keV, $2^+ \rightarrow 0^+$ transition (produced in natural Fe), with that from the ENDF/B-VI evaluated data for the total inelastic cross section for ^{56}Fe [32]. Because a very large fraction of the inelastic decay passes through the $2^+ \rightarrow 0^+$ transition, these two quantities are expected to be similar, and the evaluation is based on a large amount of data and on model calculations as well. Although there is agreement between the shape of the ENDF/B-VI curve and our excitation function, the ENDF/B-VI evaluation indicates smaller cross sections than our measurement. This is consistent with the observation in the recent evaluation [31] that the ENDF/B-VI evaluation has a lower cross section than the new evaluation. This discrepancy will be the subject of a future publication.

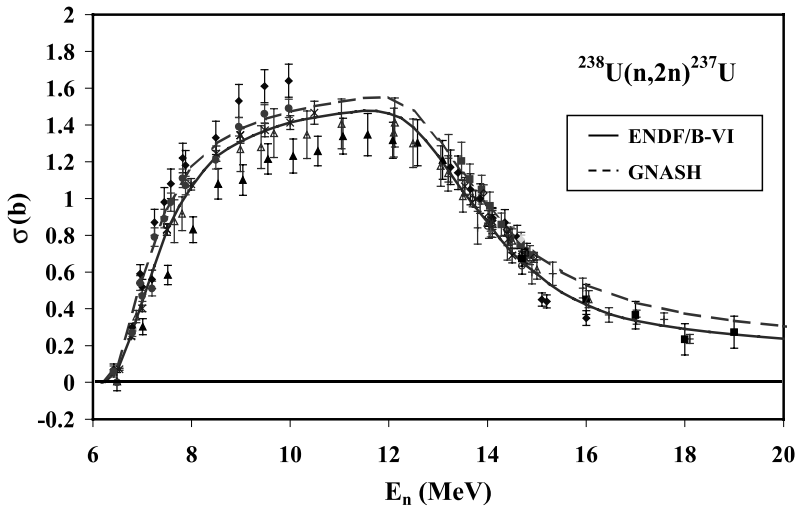

FIG. 5. Experimental data [26] (points), evaluation [25] (solid line), and GNASH calculation (dashed line) for the ^{238}U$(n, 2n)^{237}$U channel cross section.

B. Comparison with GNASH calculations

In Fig. 4 the absolute cross sections deduced in this work for the γ-ray transitions of the U isotopes in Fig. 3 are compared with cross-section predictions from GNASH calculations [24] up to E_n=30 MeV. In the ^{238}U(n, n') reaction channel the experimental cross sections for the yrast transitions do not decrease as rapidly as the calculated cross sections for $E_n > 10$ MeV for the 103.5-keV and 158.5-keV transitions [see Figs. 4(i) and 4(vi)]. Hence, it is necessary to increase the population of the lower spin yrast states at higher neutron energies. As mentioned previously, the contribution of secondary scattering effects within the target to the cross section at high neutron energies is calculated to be small, and hence, cannot account for the observed differences at neutron energies above 10 MeV.

In the $(n, 3n)$-exit channel, GNASH overestimates the cross sections for the transitions of the ground-state band and tends to underestimate the cross sections for the side-feeding transitions [compare cross sections in Figs. 4(ii), 4(vii), 4(ix), and 4(xi), with the cross sections for the 687.6-keV and 966.9-keV transitions—second peaks in the cross sections in Figs. 4(xv) and 4(xxvii). Hence, shifting part of the $(n, 3n)$-exit channel cross section from the yrast to off-yrast transitions in the calculations will probably give better agreement with the experimental data. However, the spectroscopy of the off-yrast states in ^{236}U is not as complete as that in ^{238}U and many states still remain unobserved. This presently renders incomplete any approach based on the technique of γ-ray spectroscopy alone. Hence, an extensive knowledge of the low-lying level scheme of ^{236}U will help considerably toward this end. Adjusting the calculations to shift part of the cross section from the $(n, 3n)$-exit channel to the $(n, 2n)$-exit and/or $(n, 4n)$-exit channels, while preserving the total cross section, is unlikely to give better agreement because these channels peak at different neutron energies than the $(n, 3n)$ channel. Because GNASH calculates a $(n, 3n)$ cross section that appears somewhat large, we have scaled the GNASH $(n, 3n\gamma)$ cross section calculations by the ratio of the ENDF/B-VI [25] to GNASH $(n, 3n)$ channel cross sections to provide a comparison in which the scaled calculations more closely match the available $(n, 3n)$ data. These scaled partial cross sections are plotted as dashed curves in Figs. 4(ii), 4(vii), 4(ix), and 4(xi). Note that the scaled calculations still over-

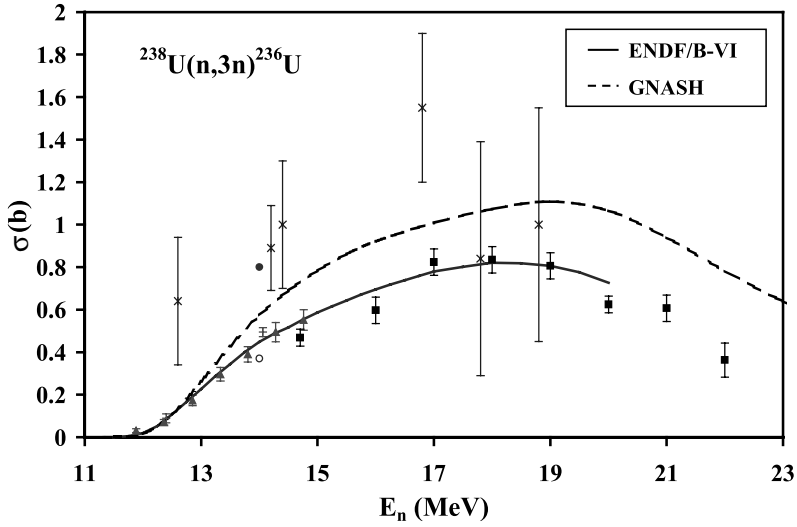

FIG. 6. Experimental data [27] (points), evaluation [25] (solid line) and GNASH calculation (dashed line) for the ^{238}U$(n, 3n)^{236}$U channel cross section.

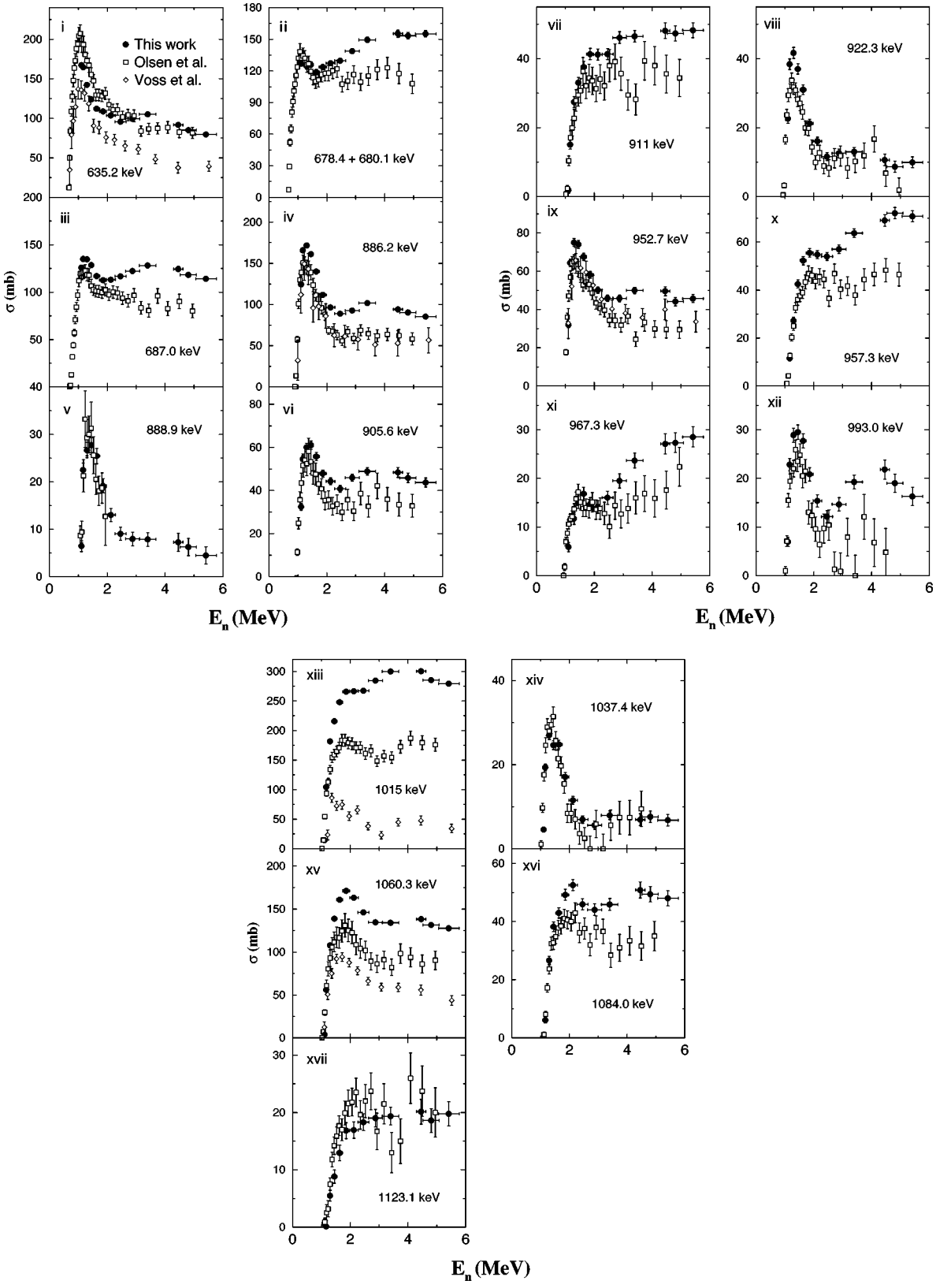

FIG. 7. Comparison between γ-ray cross sections obtained in the present work and from results reported by Olsen *et al.* [18] and Voss *et al.* [19].

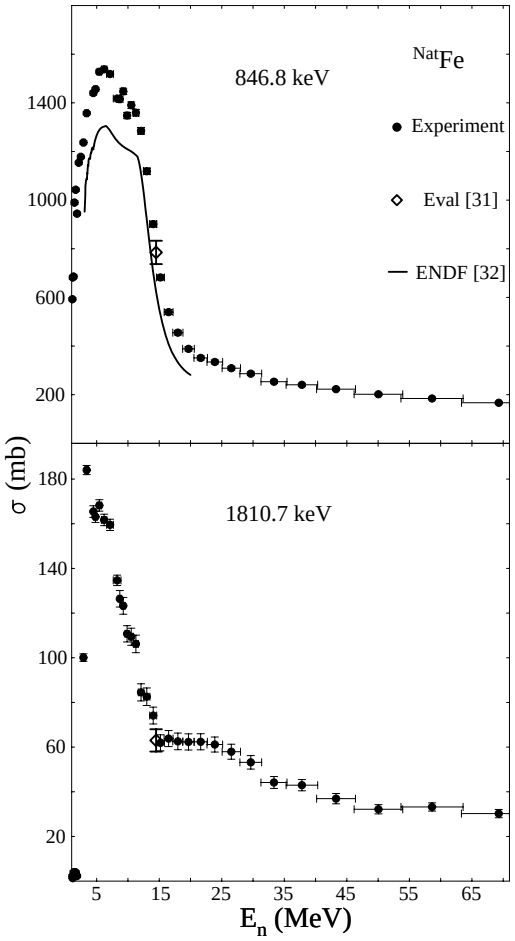

FIG. 8. Absolute cross-section values as a function of incident neutron energy for the 846.8-keV (upper part) and 1810.7- keV (lower part) transitions of ^{56}Fe in natural Fe. The open diamonds are taken from an evaluation at 14.5 MeV neutron energy [31] based on 21 and 11 studies, for 846.8 keV and 1810.7-keV transitions, respectively. In the upper part the ENDF [32] evaluated inelastic channel cross section for ^{56}Fe (solid line—values decreased by 8% to account for the percentage of ^{56}Fe in natural Fe) is plotted.

predict the observed yields, but now by some 20% to 50% instead of about 100%.

In the two- and four-neutron channels, GNASH underestimates the two transitions observed in the former channel [see Figs. 4(iii) and 4(v)] and overestimates one transition observed in the latter channel [see Fig. 4(iv)], although backgrounds, probably from fission fragments, make direct comparison with calculations of the $(n, 2n)$ cross sections difficult. These transitions represent only a small fraction of the cross section for these channels, and, hence, no general conclusions can be drawn for these channels, other than that the excitation function shapes agree well.

In many cases in Fig. 4, the shape of the experimentally observed excitation function is similar to the corresponding model prediction, while in other cases there are differences in the magnitude of the cross sections only [see, for instance, the case of the 1437.1- and 1485-keV transitions in Figs. 4(xxxv) and 4(xxxvi)]. However, in certain cases large differences in the shape of the cross-section curves are observed, such as the 931.5-keV and 962.0-keV γ rays in Figs. 4(xxii) and 4(xxvi); these may be due to contamination of the peaks from unidentified sources (for example, γ rays originating from one or more of the higher-yield fission fragments produced in the fission of ^{238}U).

The 911.9-, 1015.3-, and 1060.3-keV transitions [see Figs. 4(xx), 4(xxix), and 4(xxxi)] originate from the same level (at 1060.3 keV excitation energy, $J^{\pi}=2^{+}$). Using the known branching ratios for these three transitions [33], a deconvolution of the contributions of the 911.9- and 1015.3 -keV transitions in the total cross sections reported in Figs. 4(xx) and 4(xxix) is possible. However, the resulting cross sections, when compared to the cross section observed for the 1060.3–keV transition, are not in agreement with the known branching ratios indicating that this is a more complicated case involving perhaps contamination from additional unknown transitions. The use of coincidences between γ rays, by allowing gating on known transitions belonging to a particular isotope, would help to reduce or even eliminate contamination from overlapping γ rays in the data. But the statistics for γ-γ coincidences in the present experiment were insufficient to remove these issues of overlap.

To deduce the inelastic channel cross section from the present data and calculations, 16 γ-ray transitions (103.5, 635.2, 680.1, 687, 886.2, 905.6, 922, 931.5, 952.7, 993.0, 1015, 1037.4, 1060.3, 1084.0, 1437.1, and 1485 keV) of ^{238}U were used. These transitions feed in parallel the ground state and the first 2^{+} state of ^{238}U (see Fig. 3), hence, their absolute cross sections contribute independently to the inelastic channel cross section. By summing the absolute cross sections for these transitions, part of the cross section observed for the ^{238}U(n, n') reaction channel is obtained (see Fig. 9). Above 10 MeV neutron energy the cross sections for the 687-, 922-, 952.7-, 993.0-, and 1084.0-keV transitions have not been included in the sum due to obvious contamination from other reactions present at these neutron energies for these transitions. In Fig. 9 the sum of the GNASH predictions for these transitions is included together with the GNASH prediction for the ^{238}U(n, n')-channel cross section. The experimental points are higher than the GNASH predictions by about 20% in the energy range above about 4 MeV, and account for approximately 70% of the predicted reaction channel cross section for 2 MeV$\lesssim E_n \lesssim$7 MeV. Moreover, the inelastic channel cross section deduced from the present data corrected using the GNASH predictions is included. The correction is done by multiplying the experimental points at each neutron energy with the ratio of the GNASH prediction for the channel cross section divided by the GNASH prediction for the sum of the 16 transitions at the same neutron energy. For $E_n \gtrsim 7$ MeV, the underestimation of the cross section from the calculations, as mentioned previously, results in the experimental points rising higher than the channel cross section. It may be that the direct inelastic scattering and/or the level density and decay modeling in the GNASH calculations tend to underpredict the inelastic channel cross section. However, we cannot completely rule out the possibility that some portion of the higher-energy cross section results from experimental effects such as contributions from reactions other than inelastic scattering. Similar effects have

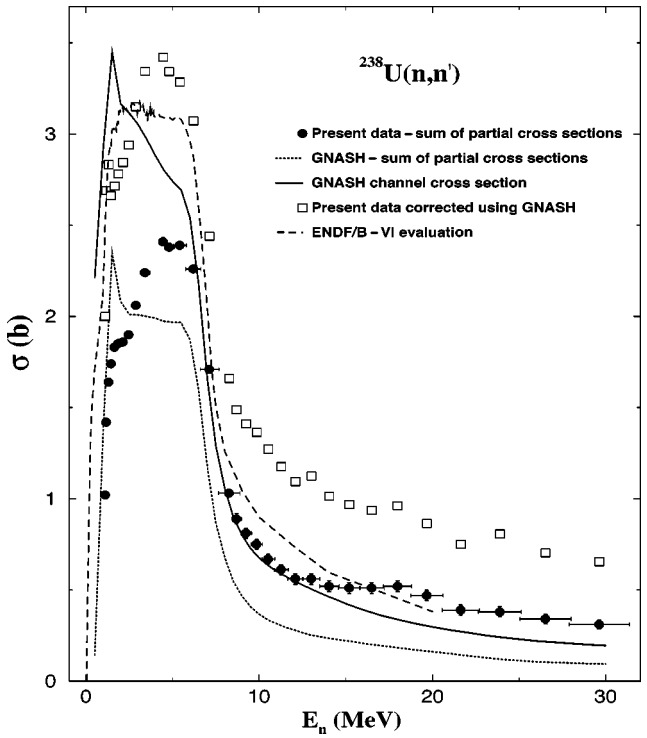

FIG. 9. Summed cross section (filled circles) for the 103.5-, 635.2-, 680.1-, .687-, 886.2-, 905.6-,.922-, 931.5-, 952.7-, 993.0-, 1015-, 1037.4-, 1060.3-, 1084.0-, 1437.1-, and 1485-keV transitions (see Fig. 3) of ^{238}U. Above 10 MeV neutron energy the cross sections for the 687-, 922-, 952.7-, 993.0-, and 1084.0-keV transitions have not been included in the sum due to obvious contamination from other reactions present at these neutron energies for these transitions. The dotted and solid lines are the GNASH predictions for the sum of these transitions and for the ^{238}U(n,n')-channel cross section, respectively. The open squares show the inelastic channel cross section deduced from the data and calculations (see text). The ENDF/B-VI [25] evaluated cross section (dashed line) is shown for comparison with the deduced cross section.

been observed in our other datasets on ^{239}Pu [10] and ^{196}Pt [13], for example.

The evaluated inelastic channel cross section from ENDF/B-VI is also shown in Fig. 9. The evaluation does not show the peak structures observed in our data at low incident neutron energies, and, like the GNASH calculation, the evaluation values at incident neutron energies above 10 MeV are about a factor of 2 lower than our deduced channel cross section. Because the neutron elastic scattering cross section is usually deduced from the measured neutron total scattering cross section and the sum of inelastic and nonelastic reactions, this result, if correct, requires substantial changes in the evaluation.

C. Population of the $K^{\pi}=4^{-}$ state

One state of special interest is the first 4^{-} level that has been identified as a two-neutron quasiparticle state with a Nilsson configuration of $\nu\frac{7}{2}[743]+\nu\frac{1}{2}[631]$ [34,35]. In the even-even isotones ^{236}U and ^{238}Pu, the two-neutron quasiparticle $K^{\pi}=4^{-}$ state is expected to lie lower than any other two-quasiparticle state, because the neutron states involved are ground states of the odd-A neighbors [36]. Below we discuss the observed population of these states in the previously reported ^{239}Pu$(n,2n)^{238}$Pu [10] reaction data and in the present ^{238}U$(n,3n)^{236}$U reaction results in relation to their nuclear structure.

In the case of ^{239}Pu$(n,2n)^{238}$Pu, a strong population of the (4^{-}), 8.5-ns, 1082.57-keV state was observed [10] with a prominent $(4^{-})\rightarrow 4^{+}$ decay transition. The strong population of the (4^{-}) state likely arises from K conservation constraining the feeding. The reported branching ratios show most of the decay (91.4%) in the $(4^{-})\rightarrow 4^{+}$ transition with very little in the decays to the 3^{-}(5.2%), (5^{-})(2.0%), and (2^{-})(1.4%) levels. This level accounts for about 14% of the ^{239}Pu$(n,2n)^{238}$Pu cross section at $E_n=10$ MeV and thus carries considerable weight in the determination of the channel cross section.

In the present case of ^{238}U$(n,3n)^{236}$U, a similar $(4)^{-}$ two-neutron quasiparticle excitation is known in ^{236}U at 1052.89 keV with a lifetime of 100 ns. However, the nuclear structure in ^{236}U is sufficiently different from ^{238}Pu that, rather than one strong $(4)^{-}\rightarrow 4^{+}$ transition, the decay intensity is spread among four transitions, $(4)^{-}\rightarrow 3^{-}$(38.3%), $(4)^{-}\rightarrow 5^{-}$ (42.4%), and $(4)^{-}\rightarrow 2^{-}$ (1.6%), with only 17.6% of the total intensity in the $(4)^{-}\rightarrow 4^{+}$ transition. Both the fragmenting of the decay strength among different γ rays and the longer lifetime of the state (that spreads out the intensity in our time spectrum, hence distorting the neutron energy dependence of the excitation function) make it difficult to observe these γ rays. Indeed, we only observe the 308-keV, $(4)^{-}\rightarrow 3^{-}$ transition with a peak cross section of approximately 12 mb. From the known branching ratios we calculate a channel cross section of about 30 mb for the population of this state, which corresponds to only 1.5% of the total $(n,3n)$ observed γ-ray decay in contrast to the ^{238}Pu case. Because all decays from the 4^{-} state in ^{236}U pass through the measured $4^{+}\rightarrow 2^{+}$ decay, the unobserved 4^{-} decay strength is contained in the $(n,3n)$ channel cross section determination. Because of the small contribution to the total, no correction for the 100 ns lifetime of this state was made in determining the $(n,3n)$ channel cross section. Another possible 4^{-} state is identified in ^{236}U at an excitation energy of 1070.0 keV. We also measured decay from this state with a peak partial cross section of 50 mb [about 2.5% of the total $(n,3n)$ decay intensity observed].

Despite the fact that the ^{238}U$(n,3n)$ reaction is expected on average to populate states of higher spin than the ^{239}Pu$(n,2n)$ reaction (due to the low average angular momenta of evaporated neutrons), we observe less population of the $K^{\pi}=4^{-}$ state in ^{236}U than in ^{238}Pu. Indeed, despite their very similar band structures, we see less side feeding in ^{236}U than in ^{238}Pu, however, it is not possible to establish the reason for this difference from the limited set of γ-ray transitions observed in these datasets. K conservation is still consistent with the ^{238}Pu data, however, K conservation in actinide nuclei deserves more study.

VI. SUMMARY

Partial ^{238}U$(n,xn\gamma)^{238-x}$U, $x\leqslant 4$, cross sections for 45 transitions have been measured for neutron energies

1 MeV $< E_n <$ 100 MeV. The results are compared with previous experimental results for γ-ray cross sections from inelastic scattering of neutrons up to $E_n \sim 6$ MeV on ^{238}U and with theoretical calculations up to $E_n = 30$ MeV from the GNASH reaction model. Agreement between experimental results and theoretical predictions was established in many cases while the differences observed provide valuable feedback for future calculations on the same or similar reactions. The small fraction of the $(n, 2n)$ and $(n, 4n)$ channel cross sections observed shows that partial γ-ray cross sections are generally not useful for determining reaction channel cross sections leading to odd-mass actinide products. The deduced inelastic channel cross section differs significantly from calculations and evaluations at incident neutron energies greater than about 10 MeV.

ACKNOWLEDGMENTS

This work has been supported by the U.S. Department of Energy under Contract Nos. W-7405-ENG-36 (LANL) and W-7405-ENG-48 (LLNL). This work has benefitted from the use of the LANSCE accelerator facility, supported under DOE Contract No. W-7405-ENG-36.

[1] D. C. Larson, in *Proceedings of the International Conference on Nuclear Data for Basic and Applied Science*, edited by P. G. d Young R. E. Brown,G. F. Auchampaugh,P. W. Lisowski, andL. Stewart (Santa Fe, NM, 1985), Vol. 1, p. 71.

[2] H. Vonach, A. Pavlik, M. B. Chadwick, R. C. Haight, R. O. Nelson, S. A. Wender, and P. G. Young, Phys. Rev. C **50**, 1952 (1994).

[3] A. Pavlik, H. Hitzenberger-Schauer, H. Vonach, M. B. Chadwick, R. C. Haight, R. O. Nelson, and P. G. Young, Phys. Rev. C **57**, 2416 (1998).

[4] R. O. Nelson, M. B. Chadwick, A. Michaudon, and P. G. Young, Nucl. Sci. Eng. **138**, 105 (2001).

[5] R. O. Nelson and A. Michaudon, Nucl. Sci. Eng. **140**, 1 (2002).

[6] J. A. Becker and R. O. Nelson, Nucl. Phys. News **7**, 11 (1997).

[7] F. S. Stephens, in *Proceedings of the International Symposium on In-Beam Nuclear Spectroscopy*, edited by Zs. Dombradi and T. Fenyes (Debrecen, Hungary, 1984), p. 205.

[8] W. Younes, J. A. Becker, L. A. Bernstein, P. E. Garrett, C. A. McGrath, D. P. McNabb, R. O. Nelson, M. Devlin, N. Fotiades, and G. D. Johns, Lawrence Livermore National Laboratory Report UCRL-ID-140313, 2000.

[9] N. Fotiades, G. D. Johns, R. O. Nelson, M. B. Chadwick, M. Devlin, W. S. Wilburn, P. G. Young, D. E. Archer, J. A. Becker, L. A. Bernstein, P. E. Garrett, C. A. McGrath, D. P. McNabb, and W. Younes, Los Alamos National Laboratory Report LA-UR-01-4281, 2001.

[10] L. A. Bernstein, J. A. Becker, P. E. Garrett, W. Younes, D. P. McNabb, D. E. Archer, C. A. McGrath, H. Chen, W. E. Ormand, M. A. Stoyer, R. O. Nelson, M. B. Chadwick, G. D. Johns, W. S. Wilburn, M. Devlin, D. M. Drake, and P. G. Young, Phys. Rev. C **65**, 021601(R) (2002).

[11] N. Fotiades, G. D. Johns, R. O. Nelson, M. B. Chadwick, M. Devlin, W. S. Wilburn, P. G. Young, D. E. Archer, J. A. Becker, L. A. Bernstein, C. A. McGrath, P. E. Garrett, D. P. McNabb, and W. Younes, J. Nucl. Sci. Technol. Supplement **2**, 234 (2002).

[12] L. A. Bernstein, J. A. Becker, W. Younes, D. E. Archer, K. Hauschild, G. D. Johns, R. O. Nelson, W. S. Wilburn, and D. M. Drake, Phys. Rev. C **57**, R2799 (1998).

[13] E. Tavukcu, L. A. Bernstein, K. Hauschild, J. A. Becker, P. E. Garrett, C. A. McGrath, D. P. McNabb, W. Younes, M. B. Chadwick, R. O. Nelson, G. D. Johns, and G. E. Mitchell, Phys. Rev. C **64**, 054614 (2001).

[14] E. Tavukcu, L. A. Bernstein, K. Hauschild, J. A. Becker, P. E. Garrett, C. A. McGrath, D. P. McNabb, W. Younes, P. Navratil, R. O. Nelson, G. D . Johns, G. E. Mitchell, and J. A. Cizewski, Phys. Rev. C **65**, 064309 (2002).

[15] P. E. Garrett, L. A. Bernstein, J. A. Becker, K. Hauschild, C. A. McGrath, D. P. McNabb, W. Younes, E. Tavukcu, G. D. Johns, R. O. Nelson, W. S. Wilburn, and S. W. Yates, Phys. Rev. C **62**, 014307 (2000).

[16] P. E. Garrett, L. A. Bernstein, J. A. Becker, K. Hauschild, C. A. McGrath, D. P. McNabb, W. Younes, M. B. Chadwick, G. D. Johns, R. O. Nelson, W. S. Wilburn, E. Tavukcu, and S. W. Yates, Phys. Rev. C **62**, 054608 (2000).

[17] P. W. Lisowski, C. D. Bowman, G. J. Russell, and S. A. Wender, Nucl. Sci. Eng. **106**, 208 (1990).

[18] D. K. Olsen, G. L. Morgan, and J. W. McConnell, ORNL Report TM-6832 1979; EXFOR retrieval by Accession No. 10909.

[19] F. Voss, S. Cierjacks, D. Erbe, and G. Schmatz, Kernforschungszentrum Karlsruhe Report 2379, 1976; EXFOR retrieval by Accession No. 21157.

[20] S. A. Wender, S. Balestrini, A. Brown, R. C. Haight, C. M. Laymon, T. M. Lee, P. W. Lisowski, W. McCorkle, R. O. Nelson, and W. Parker, Nucl. Instrum. Methods Phys. Res. A **336**, 226 (1993).

[21] R. O. Nelson, personal communication (2003).

[22] J. F. Briesmeister, LANL Report LA-12625-M, 1997.

[23] D. P. McNabb, LLNL Report UCRL-ID-139906, 2000.

[24] P. G. Young, E. D. Arthur, and M. B. Chadwick, LANL Report LA-12343-MS, 1992; P. G. Young and M. B. Chadwick (private communication).

[25] L. W. Weston, P. G. Young, and W. P. Poenitz, ORNL, LANL, Evaluated Nuclear Data Files, ENDF/B-VI evaluation, MAT No. 9237 MOD 4, February 1997; data retrieved from the ENDF database, Brookhaven National Laboratory (see http://www.nndc.bnl.gov/nndc/endf).

[26] L. Rosen *et al.*, Los Alamos Laboratory Report, LA-2111, 1957; J. D. Knight, R. K. Smith, and B. Warren, Phys. Rev. **112**, 259 (1958); J. F. Perkin and R. F. Coleman, J. Nucl. Energy, Parts A/B **14**, 69 (1961); D. Barr (private communication); D. S. Mather and L. F. Pain, Report AWRE-O-47, 1969; D. S. Mather, P. F. Bampton, R. E. Coles, G. J. James, and P. J. Nind, Report AWRE-O-72, 1972; J. H. Landrum, R. J.

Nagle, and M. Lindner, Phys. Rev. C **8**, 1938 (1973); L. R. Veeser and E. D. Arthur, in *Proceedings of the International Conference on Neutron Physics and Nuclear Data*aid (Harwell, UK, 1978), p. 1054; Chou You-Pu, Institute of Atomic Energy, Beijing, Report HSJ-77091, 1978; H. Karius, A. Ackermann, and W. Scobel, J. Phys. G **5**, 715 (1979); J. Frehaut, A. Bertin, R. Bois, and J. Jary, Accession No. 20416 021, CSISRS database, http://www.nndc.bnl.gov/; J. Frehaut, A. Bertin, and R. Bois, Nucl. Sci. Eng. **74**, 29 (1980); N. V. Kornilov, B. V. Zhuravlev, O. A. Sal'nikov, P. Raics, S. Nagy, S. Daroczy, K. Sailer, and J. Csikai, Rossendorf Report 410, 68, 1980; T. B. Ryves and P. Kolkowski, J. Phys. G **6**, 771 (1980); R. Pepelnik, B. Anders, and B. M. Bahal, in *Proceedings of the International Conference on Nuclear Data for Basic and Applied Science*, edited by P. G. Young, R. E. Brown, G.F.Auschampaugh, P. W.Lisowski, and L. Stewart (Santa Fe, NM, 1985), Vol. 1, p. 211; V. Ya. Golovnya, K. S. Goncharov, G. P. Dolya, V. A. Kuz'menko, S. G. Pasechnik, and V. V. Remaev, Accession No. 40997 002, 003, CSISRS database, http://www.nndc.bnl.gov/; A. A. Filatenkov, S. V. Chuvaev, V. N. Aksenov, V. A. Yakovlev, A. V. Malyshenkov, S. K. Vasil'ev, M. Avrigeanu, V. Avrigeanu, D. L. Smith, Y. Ikeda, A. Wallner, W. Kutschera, A. Priller, P. Steier, H. Vonach, G. Mertens, and W. Rochow, Khlopin Radiev. Inst. Leningrad Report 252, 1999.

[27] L. Rosen *et al.*, Los Alamos Laboratory Report No. LA-2111, 1957; K. W. Allen, P. Bomyer, and J. L. Perkin, J. Nucl. Energy **14**, 100 (1961); P. H. White, *ibid.* **16**, 261 (1962); D. S. Mather and L. F. Pain , Aldermaston Report AWRE-O-47, 1969; D. S. Mather, P. F. Bampton, R. E. Coles, G. J. James, and P. J. Nind, Aldermaston Report AWRE-O-72, 1972; L. R. Veeser and E. D. Arthur, in *Proceedings of the International Conference on Neutron Physics and Nuclear Data* (Harwell, UK, 1978), p. 1054; J. Frehaut, A. Bertin, R. Bois, and J. Jary, Accession No. 20416 022, CSISRS database, http://www.nndc.bnl.gov

[28] *Reference Input Parameter Library for Theoretical Calculations of Nuclear Reactions*, Handbook for Calculations of Nuclear Reaction Data Vol. 1, available at http://iaeand.iaea.or.at/

[29] A. Jensen, in *Proceedings of the International Conference on Nuclear Physics and Nuclear Data* (Harwell, UK, 1978), p. 378.

[30] P. G. Young and M. B. Chadwick, Los Alamos Laboratory Report No. T-16-MPY12, 2000 (unpublished).

[31] S. P. Simakov, A. Pavlik, H. Vonach, and S. Hlaváč, Report INDC(CCP)-413, 1998.

[32] Evaluated Nuclear Data Files, ENDF/B-VI evaluation, MAT No. 2631 MOD 4, May 2000; data retrieved from the ENDF database, Brookhaven National Laboratory (see http://www.nndc.bnl.gov/nndc/endf).

[33] F. K. McGowan and W. T. Milner, Nucl. Phys. **A571**, 569 (1994).

[34] B. Bengtson, J. Jensen, M. Moszynski, and H. L. Nielsen, Nucl. Phys. **A159**, 249 (1970).

[35] K. Katori, A. M. Friedman, and J. R. Erskine, Phys. Rev. C **8**, 2236 (1973).

[36] V. G. Soloviev and T. Siklos, Nucl. Phys. **59**, 145 (1964).